3-13-2014

The Wnt/Planar Cell Polarity Pathway Component Vangl2 Induces Synapse Formation through Direct Control of N-Cadherin

Tadahiro Nagaoka
Niigata University

Riuko Ohashi
Niigata University

Ayumu Inutsuka
Niigata University

Seiko Sakai
Niigata University

Nobuyoshi Fujisawa
Niigata University

See next page for additional authors

Cell Reports
Article

The Wnt/Planar Cell Polarity Pathway Component Vangl2 Induces Synapse Formation through Direct Control of N-Cadherin

Tadahiro Nagaoka,[1] Riuko Ohashi,[2] Ayumu Inutsuka,[1] Seiko Sakai,[3] Nobuyoshi Fujisawa,[3] Minesuke Yokoyama,[3] Yina H. Huang,[4] Michihiro Igarashi,[5] and Masashi Kishi[1,*]
[1]Laboratory of Molecular Neuroimaging, Graduate School of Medical and Dental Sciences, Niigata University, Niigata 951-8510, Japan
[2]Division of Cellular and Molecular Pathology, Graduate School of Medical and Dental Sciences, Niigata University, Niigata 951-8510, Japan
[3]Department of Comparative and Experimental Medicine, Brain Research Institute, Niigata University, Niigata 951-8510, Japan
[4]Departments of Pathology and Microbiology and Immunology, The Geisel School of Medicine at Dartmouth, Hanover, NH 03755-1404, USA
[5]Department of Neurochemistry and Molecular Cell Biology, Graduate School of Medical and Dental Sciences, Niigata University, Niigata 951-8510, Japan
*Correspondence: masashi.kishi@gmail.com
http://dx.doi.org/10.1016/j.celrep.2014.01.044

SUMMARY

Although regulators of the Wnt/planar cell polarity (PCP) pathway are widely expressed in vertebrate nervous systems, their roles at synapses are unknown. Here, we show that Vangl2 is a postsynaptic factor crucial for synaptogenesis and that it coprecipitates with N-cadherin and PSD-95 from synapse-rich brain extracts. Vangl2 directly binds N-cadherin and enhances its internalization in a Rab5-dependent manner. This physical and functional interaction is suppressed by β-catenin, which binds the same intracellular region of N-cadherin as Vangl2. In hippocampal neurons expressing reduced Vangl2 levels, dendritic spine formation as well as synaptic marker clustering is significantly impaired. Furthermore, Prickle2, another postsynaptic PCP component, inhibits the N-cadherin-Vangl2 interaction and is required for normal spine formation. These results demonstrate direct control of classic cadherin by PCP factors; this control may play a central role in the precise formation and maturation of cell-cell adhesions at the synapse.

INTRODUCTION

Synapse formation in the CNS is mediated by intercellular communication between axonal growth cones and the soma or dendrites of their target neurons. Small knot-like protrusions referred to as dendritic spines are formed on the postsynaptic side of the excitatory synapses (Segal, 2005). By regulating the synthesis, transport, and activity of the synaptic proteins within, spines function as one of the storage sites of synaptic strength where the efficacy of the neurotransmission can be potentiated or depressed for learning and memory (Okabe, 2012). The number of spines correlates with brain function. For example, their densities are drastically reduced in the brain tissues of humans or mice with dementia (Ferrer and Gullotta, 1990; Perez-Cruz et al., 2011). Characterization of molecules that control spine formation will therefore illuminate the cell biological basis of memory formation and loss (Yoshihara et al., 2009).

Synaptic cell adhesion molecules cooperatively modulate the membrane interactions required for spine formation. One such critical player is N-cadherin, a calcium-dependent homophilic cell adhesion molecule predominantly expressed in the nervous system (Arikkath and Reichardt, 2008; Takeichi and Abe, 2005; Togashi et al., 2002). N-cadherin is linked to the actin cytoskeleton through β-catenin whose regulated distribution is required for spine morphogenesis (Murase et al., 2002). Catenins support spine formation by clustering cadherin molecules and inhibiting their internalization from the cell surface (Le et al., 1999). Although postsynaptic N-cadherin is endocytosed at a high rate (Tai et al., 2007), the molecular nature of the driving force for this internalization is unknown.

Wnt signaling plays diverse roles in animal development and is divided into canonical and noncanonical pathways (Wallingford and Habas, 2005). Noncanonical signaling involves several intracellular pathways that act independently of β-catenin and regulate cytoskeletal dynamics and cell adhesion (Wallingford and Habas, 2005). The noncanonical Wnt/planar cell polarity (PCP) pathway functions similar to the *Drosophila* PCP pathway through Frizzled (Fz) and Dishevelled (Dvl) to activate Rho and Rac small GTPases. In this pathway, the Strabismus/Van Gogh-Prickle protein complex antagonizes Fz-Dvl signaling. As for the regulation of cell-cell adhesion, the noncanonical Wnt ligand Wnt11 controls the cell surface level of E-cadherin through Rab5c-dependent endocytosis in zebrafish gastrulation (Ulrich et al., 2005). However, the molecular mechanism by which the noncanonical Wnt signaling regulates endocytosis of classic cadherin remains obscure.

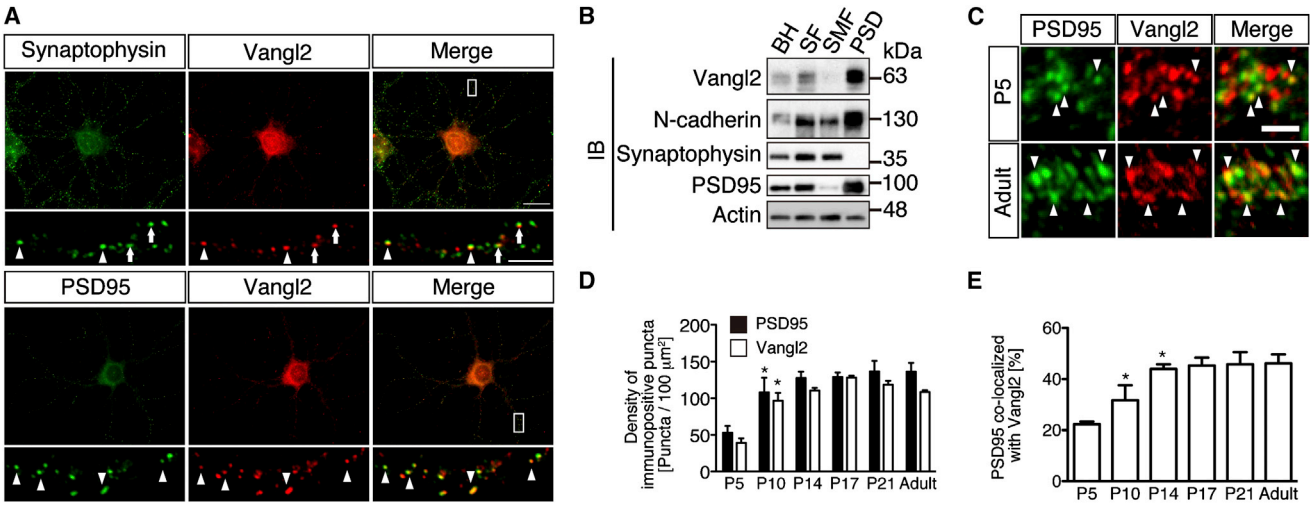

Figure 1. Vangl2 Is a Postsynaptic Factor of the CNS Synapse

(A) Vangl2 (red) colocalizes with the synaptic markers (green) in cultured hippocampal neurons (synaptophysin: 42.5%, n = 106; PSD-95: 61.7%, n = 94, from four images in one representative experiment for each). Note that Vangl2 is slightly misaligned with the presynaptic marker at some puncta (arrows). The α-Vangl2 Abs were diluted 1:200 for IF. The signal using a 1:1,000 dilution was too faint to obtain clear images.

(B) WB analysis of Vangl2 distribution in the subfractionated brain samples. BH, brain homogenate; SF, synaptosomal fraction; SMF, synaptic membrane fraction; PSD, postsynaptic density. Ten micrograms of protein from each fraction was analyzed using α-Vangl2, N-cadherin, Synaptophysin, PSD-95, and β-actin Abs.

(C) Synaptic localization of Vangl2 in the neonatal (P5: upper panels) and adult (P56: lower panels) mouse hippocampal CA1 region just apical to the pyramidal cell layer. Localization of PSD-95 (green), Vangl2 (red), and the merged views are shown in highly magnified images.

(D and E) Vangl2 accumulates at synapses during postnatal development. Immunopositive puncta were counted in a 100 μm^2 square and averaged (n = 10 squares from four mice for each stage). Quantification of the densities of the Vangl2- and PSD-95-positive puncta (D), and the ratio of Vangl2-positive clusters of PSD-95 (E) are shown in the bar graphs.

Data are presented as mean ± SD. Significant differences ($p < 0.05$) versus a one stage younger group calculated using Student's t test are marked with an asterisk. For identification of synapses, several examples of the colocalized puncta are indicated by arrowheads. Scale bars: (A) 20 and 5 μm for upper and lower panels, respectively, (C) 2 μm.

In vertebrate development, PCP regulates tissue morphogenesis, including establishment of the uniform orientation of cochlear hair cells, control of epidermal hair patterning, and the convergent extension movements of mesodermal and neuroectodermal cells (Wallingford and Habas, 2005). In the differentiated neurons, regulators of the Wnt/PCP pathway are required for the normal extension and guidance of growing axons (Shafer et al., 2011; Zhou et al., 2008). Here, we report another role for the PCP regulators in animal development; Vangl2 and Prickle2 (Pk2) are required for the normal development of synapses. The formation and maturation of cadherin-based cell-cell junctions at the synapse may be precisely controlled by crosstalk between the N-cadherin-β-catenin cell adhesion system and the Vangl2-Pk2 PCP complex.

RESULTS

Synaptic Protein Vangl2 Identified

Mouse homologs of core Wnt/PCP-related factors, except Vangl1, are widely transcribed in the developing nervous system (Tissir and Goffinet, 2006). To determine their role in the neural circuits, we analyzed their immunolocalizations in rat hippocampal neurons cultured for 23 days. We found that Vangl2 localized in a punctate pattern, which was speculated to be related to the synapse. As expected, Vangl2 colocalized with general synaptic markers, such as synaptophysin (Figure 1A) or SV2 (Figure S1A), and primarily with PSD-95 (Figure 1A), a postsynaptic marker of the excitatory synapse. Vangl2 also colocalized with gephyrin, an inhibitory synapse component (Figure S1A). The colocalization of Vangl2 and PSD-95 involved their physical interaction (Figure S1B). Furthermore, the synaptic immunosignals of Vangl2 were specific because they were undetectable in cells expressing small hairpin RNA (shRNA) constructs targeting the rat Vangl2 gene (Figures S1C and S1D). These results demonstrate that Vangl2 is a synaptic component of mammalian CNS, if not completely specific.

To determine the site of Vangl2 localization in a synapse, we performed western blot (WB) analysis of brain extracts, which were fractionated using sucrose density gradient centrifugation (Figure 1B) (Cohen et al., 1977). Synaptophysin, a synaptic vesicle protein localized at the presynaptic axon terminus, was enriched in the synaptic membrane fraction (SMF) and was not detectable in PSD. In contrast, postsynaptic proteins such as PSD-95 were enriched in the PSD fraction. Compared with PSD-95, Vangl2 was similarly enriched, suggesting that Vangl2 is a component of PSD. Localization of Vangl2 was distinct from that of N-cadherin (Figure 1B) that resides at the pre- and postsynaptic sides of the synapse. The specific synaptic localization of Vangl2 was confirmed by detection of GFP-Vangl2 (Devenport et al., 2011) as clusters only on the postsynaptic side of synapses (Figure S1E).

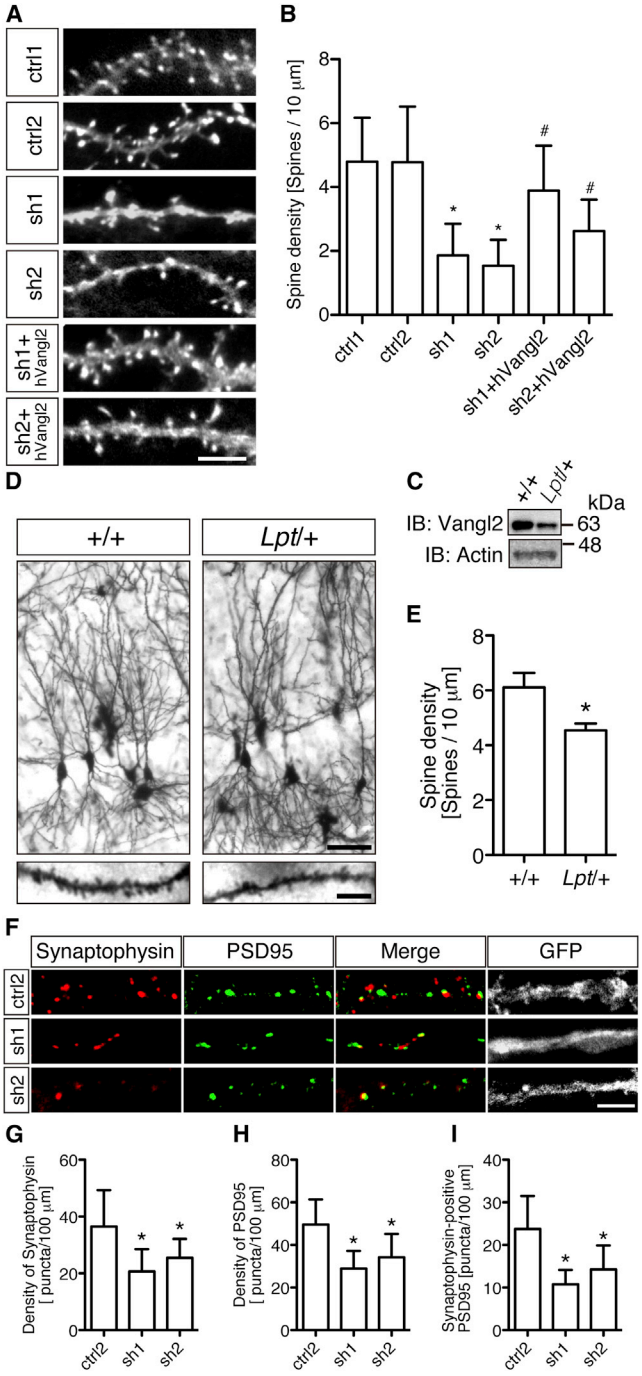

Figure 2. Role of Vangl2 in Normal Development of Dendritic Spines and Synapse Formation

(A and B) Dendritic spines of cultured rat hippocampal neurons. For quantification, actin-GFP was cotransfected with the shRNA constructs. A human cDNA (hVangl2) was cotransfected in the rescue experiments. Representative images are shown in (A), and the quantification of spine density is presented in the bar graphs (B).

(C–E) Characterization of the hippocampus of *Lpt*/+ mice. (C) WB analysis of protein samples obtained from the P4 hippocampus of wild-type and *Lpt*/+ mutant mice using actin as a loading control. Note the significant reduction of Vangl2 expression. (D) Pyramidal neurons in the hippocampal CA1 region (3 weeks old) were analyzed using Golgi's method. Low- and high-power magnifications (upper and lower panels, respectively) of dendrite images are shown. (E) Quantification of spine densities along the apical dendrites.

(F–I) Cultured hippocampal neurons fixed using methanol at 17 or 18 days in vitro (DIV) were immunostained with α-synaptophysin (red) and α-PSD-95 (green) Abs (F). Densities of puncta for the synaptic markers along the dendrites were significantly reduced in Vangl2-silenced neurons (G–I). Data for DIV17 neurons are shown.

Data are presented as mean ± SD. Significant differences ($p < 0.05$) versus control groups calculated using Student's t test are marked (*: versus ctrl2 or wild-type; #: versus sh1 or sh2, respectively). Scale bars, 5 μm (A and F), 50 μm for (D, upper panels), and 5 μm (D, lower panels).

Vangl2 is widely expressed in the adult mouse hippocampus (Figures S1F–S1H). As seen in Figures 1C and S1J, 23.9% ± 3.7% and 49.5% ± 8.8% of the Vangl2-positive puncta colocalized with PSD-95 at the apical dendrites of the neonatal (postnatal day 5, P5) and adult (P56) hippocampal CA1 region, respectively (n = 4 images for each stage. In each image, 100 puncta were counted). During development, the density of the PSD-95 puncta and the ratio of Vangl2-colocalized clusters of PSD-95 increased from P5 (53.0 ± 9.1 puncta; 22.3% ± 1.1%), P10 (108 ± 20 puncta; 31.7% ± 5.9%) to P14 (128 ± 9 puncta; 44.0% ± 1.8%), and plateaued by P17 (129 ± 6 puncta; 45.4% ± 3.1%) (Figure S1I and quantified in Figures 1D and 1E), indicating that synaptic accumulation of Vangl2 correlated with hippocampal synaptogenic activity.

Vangl2 Is Required for Normal Dendritic Spine Formation and Synaptogenesis

To determine the role of Vangl2, two shRNAs (sh1 and 2) specific for rat Vangl2 mRNA (Figure S1C) were transfected into neurons. In these neurons, the number of dendritic spines, identified as protrusions emitting GFP fluorescence, was significantly lower than that in the control shRNA (ctrl1 and 2) transfected neurons (ctrl1: 4.8 ± 1.4 spines/10 μm; ctrl2: 4.8 ± 1.7 spines/10 μm; sh1: 1.9 ± 1.0 spines/10 μm; sh2: 1.5 ± 0.8 spines/10 μm; n = 20 neurons each) (Figures 2A and 2B). The reduction of spine density was partially rescued by cotransfection with human Vangl2 cDNA (sh1 + hVangl2: 3.9 ± 1.4 spines/10 μm; sh2 + hVangl2: 2.6 ± 1.0 spines/10 μm) (Figures 2A and 2B), which was not recognized by the rat shRNAs (Figure S1C), indicating that defective spine formation was a specific consequence of reduced Vangl2 expression. Although Vangl2 regulates certain types of cell polarity, we did not observe impaired axon-dendrite polarity as shown in Figure S2, excluding the possibility that the spine phenotype is a secondary effect of the altered identity of neuronal processes.

To assess the significance of these observations, we determined whether normal spine formation in vivo requires Vangl2. A mouse strain harboring a mutation in *Vangl2* is known as *loop-tail* (*Lpt*) (Kibar et al., 2001b). Because *Lpt* homozygotes are embryonic lethal, we analyzed the hippocampi of heterozygotes. WB analysis revealed that Vangl2 expression decreased by approximately 50% compared with the wild-type (Figure 2C), consistent with results for embryonic whole brains (Guyot et al., 2011) and with the findings that the stability of mutant Vangl2 is markedly diminished (Gravel et al., 2010). Although the overall formation of neuronal processes in the hippocampus revealed

by Golgi staining was not markedly affected in the mutant (Figure 2D, upper panels), dendritic spine density was decreased (Figures 2D, lower panels, and 2E) (+/+: 6.1 ± 2.6 spines/10 μm; *lpt*/+: 4.5 ± 1.4 spines/10 μm; n = 25 neurons each). Because Vangl2 expressed from the *Lpt* allele exerts a dominant-negative effect on Vangl function (Yin et al., 2012), we conclude that formation of normal dendritic spines in vivo requires Vangl family-mediated function, as shown for Vangl2 in cultured neurons.

Because Vangl2 coprecipitated with PSD-95 (Figure S1B), we investigated whether Vangl2 regulates synapse formation by affecting synaptic marker clustering (Figure 2F) (Takahashi et al., 2011). Immunofluorescence microscopy showed that Vangl2-silenced neurons had significantly reduced density of puncta for the presynaptic marker synaptophysin (ctrl2: 36.5 ± 12.8 clusters/100 μm; sh1: 20.7 ± 7.8 clusters/100 μm; sh2: 25.5 ± 6.6 clusters/100 μm; n = 20 neurons each) (Figure 2G) as well as for the postsynaptic marker PSD-95 (ctrl2: 49.6 ± 11.7 clusters/100 μm; sh1: 28.9 ± 8.3 clusters/100 μm; sh2: 34.2 ± 11.0 clusters/100 μm; n = 20 neurons each) (Figure 2H). The density of puncta positive for both markers was also reduced (ctrl2: 23.8 ± 7.7 clusters/100 μm; sh1: 10.8 ± 3.4 clusters/100 μm; sh2: 14.3 ± 5.6 clusters/100 μm; n = 20 neurons each) (Figure 2I). These results demonstrated that Vangl2 is required for the normal synaptogenesis in the CNS.

Vangl2 Is Associated with N-Cadherin at the Synapse

To address the molecular mechanism of regulation of spine and synapse formation by Vangl2, we analyzed Vangl2-associated proteins at the synapse using coimmunoprecipitation (coIP). The purified PSD fraction was solubilized with 1% NP-40 and immunoprecipitated (IPed) with α-Vangl2 antibodies (Abs). Vangl proteins function at cell-cell junctions (Strutt and Strutt, 2007). Therefore, we determined whether synaptic adhesion molecules implicated in postsynaptic differentiation or spine formation formed immunoprecipitates (IPs) with Vangl2. Neuroligin-1 (Graf et al., 2004; Scheiffele et al., 2000) or SynCAM (Biederer et al., 2002) was not detected in the IPs, in contrast to N-cadherin (Togashi et al., 2002) (Figure 3A). The interaction was assessed using cotransfection in HEK293T cells that do not express either protein significantly (Figures 3B, 3C, S3A, and S3B). N-cadherin did not form detectable complexes with stargazin, another tetraspanin protein (Figures 3B and 3C), and neuroligins were not coIPed with Vangl2 (Figure S3C), indicating the specificity of the Vangl2-N-cadherin interaction.

We next tested whether Vangl2 mutant proteins harboring point mutations or in-frame deletions formed complexes (Figures 3D–G). Binding required the C-terminal (CT) but not the N-terminal (NT) intracellular domain (ICD) (Figures 3D and 3E, ΔCT and ΔNT). A pull-down assay using purified recombinant proteins confirmed these findings (Figure 3F). The CT of *Drosophila* Strabismus/Van Gogh includes a conserved domain that binds to Prickle (Jenny et al., 2003). Although deletion of the corresponding region of mouse Vangl2 (amino acid residues 298–382) (Figure 3D) greatly diminished the interaction (Figures 3E and 3F, ΔPkBD), *Lpt* mutations (S464N and D255E) (Kibar et al., 2001a; Kibar et al., 2001b) or deletion of the PDZ-binding motif (ΔETSV) at the CT end did not (Figure 3E). This indicates that the Prickle-binding domain is required for association with N-cadherin. Because Pk2 localizes to postsynapses (Hida et al., 2011), we determined whether it affected the N-cadherin-Vangl2 interaction. Compared with other molecules related to the Wnt/PCP pathway or canonical Wnt signaling, coexpression of Pk2 constructs greatly decreased N-cadherin-Vangl2 interaction (Figure 3G). In this experiment, Pk2 was detected in the Vangl2 IPs (Figure 3G), indicating that Pk2 affects the N-cadherin-Vangl2 interaction by binding to Vangl2. In the hippocampal neurons, expression of Pk2-shRNA (Figure S3D) reduced the density of dendritic spines (Figures 3H and 3I) (ctrl2: 4.5 ± 1.2 spines/10 μm; pk2-shRNA: 3.0 ± 0.8 spines/10 μm; n = 20 neurons for each), indicating that Pk2 is required for their normal formation, as shown for Vangl2. The PkBD of Vangl2 is important for its protein localization. In the transfected neurons, GFP-Vangl2ΔPkBD mainly distributed in the cell bodies (Figure S3E) in a granular pattern of diffusion with very few colocalization with PSD-95 in the proximal dendrites (Figure S3E, a). In the distal dendrites (Figure S3E, b), its distribution was difficult to detect. These results indicate that the synaptic localization of Vangl2 requires normal protein interaction through the PkBD.

We next identified the Vangl2-binding site within N-cadherin (Figures 4A and 4B). The ICD of cadherin harbors a juxtamembrane dileucine motif required for the lateral transport of E-cadherin (Miyashita and Ozawa, 2007). This motif is conserved in N-cadherin (amino acid residues 758 and 759) but is not required for the interaction (LL/AA). Two stretches of acidic amino acid residues (EED starting from residue 780 and ending with DD at the CT) as well as the juxtamembrane domain core region (JMDC), which are required for p120-catenin binding (Arikkath and Reichardt, 2008; Elia et al., 2006), are also dispensable (EED/AAA, ΔDD, and ΔJMDC, respectively). In contrast, the serine-rich β-catenin-binding region in N-cadherin ICD (Stappert and Kemler, 1994) is required for the interaction (β-cat. BD (S/A): serine residues within the amino acid residues from 863 to 878 are alanine substituted).

The Vangl2-N-cadherin interaction requires the β-catenin-binding site; however, whether Vangl2-N-cadherin binding occurs in concert with β-catenin or is exclusive is unknown. Because HEK293T cells abundantly express β-catenin, we first determined whether β-catenin was present in N-cadherin-Vangl2 IPs (Figures 3B and 3C). β-catenin was not detectable in IPs of FLAG-Vangl2 (Figure 3B), whereas α-N-cadherin Abs coIPed Vangl2 and β-catenin (Figure 3C). These results indicate that Vangl2-bound N-cadherin represents a subpopulation distinct from that of β-catenin-bound N-cadherin, suggesting that Vangl2 and β-catenin do not bind same N-cadherin molecule simultaneously.

To determine whether Vangl2 and β-catenin compete for the same N-cadherin-binding site, the level of endogenous β-catenin was reduced using human β-catenin-shRNAs (Firestein et al., 2008) (Figures 4C and 4D). When β-catenin levels were reduced, increased amounts of N-cadherin associated with Vangl2 were observed (sh1: 153% ± 31%; sh2: 208% ± 48%). Moreover, if the level of β-catenin was increased by coexpressing chicken β-catenin (Murase et al., 2002), the association of N-cadherin with Vangl2 decreased dose-dependently (Figures 4E and 4F; 0.2 μg of β-catenin plasmid DNA: 59.2% ± 14.4%; 0.5 μg: 47.5% ± 14.6%; 1.0 μg: 22.5% ± 8.3%). Therefore, the

Cell PRESS
Open ACCESS

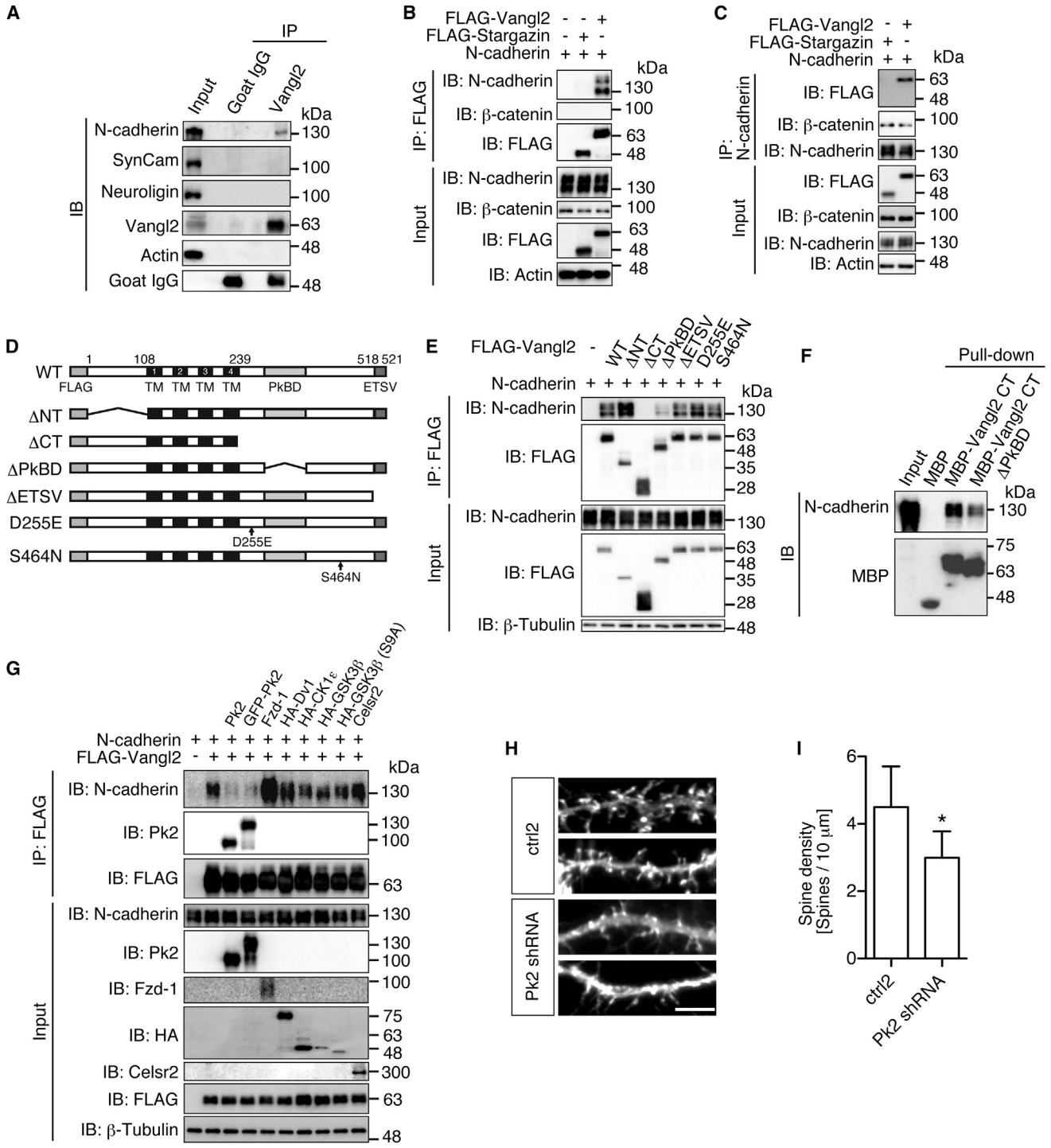

Figure 3. Vangl2 Interacts with N-Cadherin

(A) WB analysis of IPs of the PSD fraction using an α-Vangl2 Ab. Note the specific coIP of N-cadherin by the α-Vangl2 Ab. Actin was not detected in this complex, indicating that the N-cadherin-Vangl2 complex is not associated with actin filament.

(B and C) WB analysis of cell lysates IPed using α-FLAG (B) or α-N-cadherin (C) Abs. Cells were cotransfected with an N-cadherin expression vector and either FLAG-Vangl2 or FLAG-stargazin. (B) Note the absence of β-catenin in the α-FLAG IPs. (C) The coIPed level of β-catenin with α-N-cadherin Ab compared with the input level was slightly reduced by introduction of FLAG-Vangl2.

(D–F) Determination of regions of Vangl2 required for N-cadherin interaction. (D) Schematic representation of the mutant constructs. (E) Cells were cotransfected with the mutant FLAG-Vangl2 construct and wild-type N-cadherin, IPed with α-FLAG Abs, and then subjected to WB analysis with α-N-cadherin Abs to probe the

(legend continued on next page)

Vangl2-N-cadherin interaction is competitively regulated by β-catenin. We also observed a consistently reduced level of β-catenin that associated with N-cadherin in cells overexpressing Vangl2 (Figure 3C; 63.3% ± 3.1%; n = 4 experiments). Moreover, in the PSD fraction of the *Lpt*/+ mice, the level of β-catenin coIPed with α-N-cadherin Abs was conversely increased (Figures 4G and 4H; 171% ± 27%), indicating that Vangl proteins are required to regulate the N-cadherin-β-catenin interaction at the PSD, where Vangl2 is highly enriched.

Vangl2 Enhances N-Cadherin Internalization

The N-cadherin-Vangl2 interaction reflects their subcellular localization; in 53.1% of cotransfected cells (n = 64 cells from one representative experiment), they partially colocalized with intracellular vesicles (Figure 5A, green and red, respectively). Further, at the border of the N-cadherin transfectants (Figure 5B), increased vesicular localization was observed on the side with significant expression of Vangl2 (Figure 5B, b; 78.3%; n = 23 adherence sites from two representative experiments). Because N-cadherin functions at the cell surface, we hypothesized that Vangl2 is involved in N-cadherin transport and therefore determined whether coexpression of Vangl2 affected the cell-surface expression of N-cadherin.

We first used Abs against the extracellular domain (ECD) and ICD of N-cadherin (Figure S4A) (Willingham, 2010). Briefly, transfected cells were fixed using paraformaldehyde (PFA), stained with α-ECD Abs, washed extensively, permeabilized with Triton X-100, and then stained with α-ICD Abs. The Abs were detected using secondary Abs conjugated to different fluorophores, and their images were captured using the same exposure time and gain for each fluorophore. We detect N-cadherin with the α-ICD antibody (Ab) significantly only after permeabilization (Figures S4A and S4B), and α-ECD Abs did not stain intracellular pool of N-cadherin well without permeabilization (Figures S4C and S4D). The α-ECD Abs therefore did not stain the intracellular pool of the ECD epitopes at the comparable level in this experiment. By calculating the ratio of signal strengths generated by α-ECD- to that by α-ICD Abs (Figure S4B), we quantified the cell-surface expression of N-cadherin and found that it was significantly reduced by cotransfection with Vangl2 (Figure 5C; 29.2%; 95% confidence interval [CI], 26.9%–31.6%).

To further confirm the function of Vangl2, we determined the level of cell-surface N-cadherin biochemically (Figures 5D and 5E). The plasma membrane proteins were covalently labeled with biotin and enriched by precipitation using streptavidin beads (Suzuki et al., 2010). The precipitates were analyzed using WB analysis with α-N-cadherin or α-transferrin receptor (TfR) Abs as probes to quantify their cell-surface expression levels. Although the level of N-cadherin in the cell lysate was unaffected, the level of biotinylated N-cadherin was reduced by cotransfection of Vangl2 (Figures 5D and 5E; 28.6% ± 3.0%), demonstrating that expression of N-cadherin at the cell surface was negatively regulated by Vangl2. Further, the level of biotinylated TfR was unchanged in the Vangl2 transfectant (Figure 5D; 103% ± 11%), indicating specific regulation of N-cadherin by Vangl2.

The results suggest that Vangl2 is involved in cell-surface expression of N-cadherin. However, it is unknown whether Vangl2 enhances its endocytosis or inhibits exocytosis. To obtain insights into the molecular mechanism, we tested a panel of Abs raised against the constituents or regulators of intracellular vesicles to determine whether they are associated with the N-cadherin-Vangl2 complex. Rab5, a small GTPase that regulates early endosome formation and docking (Bucci et al., 1992), colocalized with the complex (Figure 5A, blue), whereas the other molecules (Figure S4F), except for Adaptin-β (Figure S4E), did not. In most of cotransfectants harboring vesicular N-cadherin-Vangl2 colocalization, we observed associated clustering of Rab5. In these cells, 71% of the N-cadherin-Vangl2-positive vesicles associated with Rab5 (n = 106 puncta). To determine the significance of the colocalization, we cotransfected these cells with a dominant-negative form of Rab5 (RFP-dnRab5) (Bohdanowicz et al., 2012) (Figures 5F and 5G). The cell-surface expression of N-cadherin was restored (Vangl2 + dnRab5: 132% ± 16%; Vangl2: 31.4% ± 17.3%), suggesting that Vangl2 affects N-cadherin transport at least in part by enhancing the Rab5-dependent endocytosis.

Cells treated with EGTA immediately endocytose E-cadherin (Le et al., 1999), which disrupts cadherin-dependent cell-cell adhesion. Here, EGTA treatment reduced the cell-surface expression of N-cadherin (Figures 5C–5E, S4A, and S4B). In this experimental condition, the N-cadherin-Vangl2 interaction transiently increased 30 min after treatment (146% ± 16%) (Figures 4I–4K). In contrast, the N-cadherin-β-catenin interaction was consistently reduced, starting immediately after addition of EGTA (5 min: 48.4% ± 12.5%). These results further indicate that molecular interaction between N-cadherin and Vangl2 is related to endocytosis of N-cadherin. Because β-catenin prevents the N-cadherin-Vangl2 interaction (Figures 4C and 4D), dissociation of β-catenin from N-cadherin may provide a binding site for Vangl2.

Because β-catenin prevents physical interaction between N-cadherin and Vangl2, we determined whether β-catenin affects the Vangl2-enhanced internalization of N-cadherin (Figures 5H and 5I). By overexpressing β-catenin, the cell-surface expression of N-cadherin reduced by Vangl2 was restored,

α-FLAG IPs. (F) A pull-down assay to determine direct binding between N-cadherin and Vangl2. Full-length N-cadherin was incubated with beads coated with purified MBP, MBP-Vangl2CT, or MBP-Vangl2CTΔPkBD. WB analysis: eluates were probed with α-N-cadherin or α-MBP Abs with 0.5% of the N-cadherin used for each pull-down as input.

(G) The effects of Wnt/PCP pathway or canonical Wnt signaling-related molecules on the N-cadherin-Vangl2 interaction. Prickle2 (Pk2, GFP-Pk2), Frizzled-1 (Fzd-1), Dishevelled-1 (HA-Dv1), Casein Kinase 1ε (HA-CK1ε), GSK3β, constitutively active form of GSK3β (HA-GSK3β [S9A]), and Celsr2 were examined. Note the specific inhibition by the Prickle2 constructs.

(H and I) Inhibition of Pk2 expression impaired formation of the dendritic spines. Actin-GFP was cotransfected with the shRNA constructs. Representative images are shown in (H), and the quantification of spine density is presented in the bar graphs (I). Scale bar, 5 μm. Data are presented as mean ± SD. Significant differences ($p < 0.05$) versus control group calculated using Student's t test are marked with an asterisk.

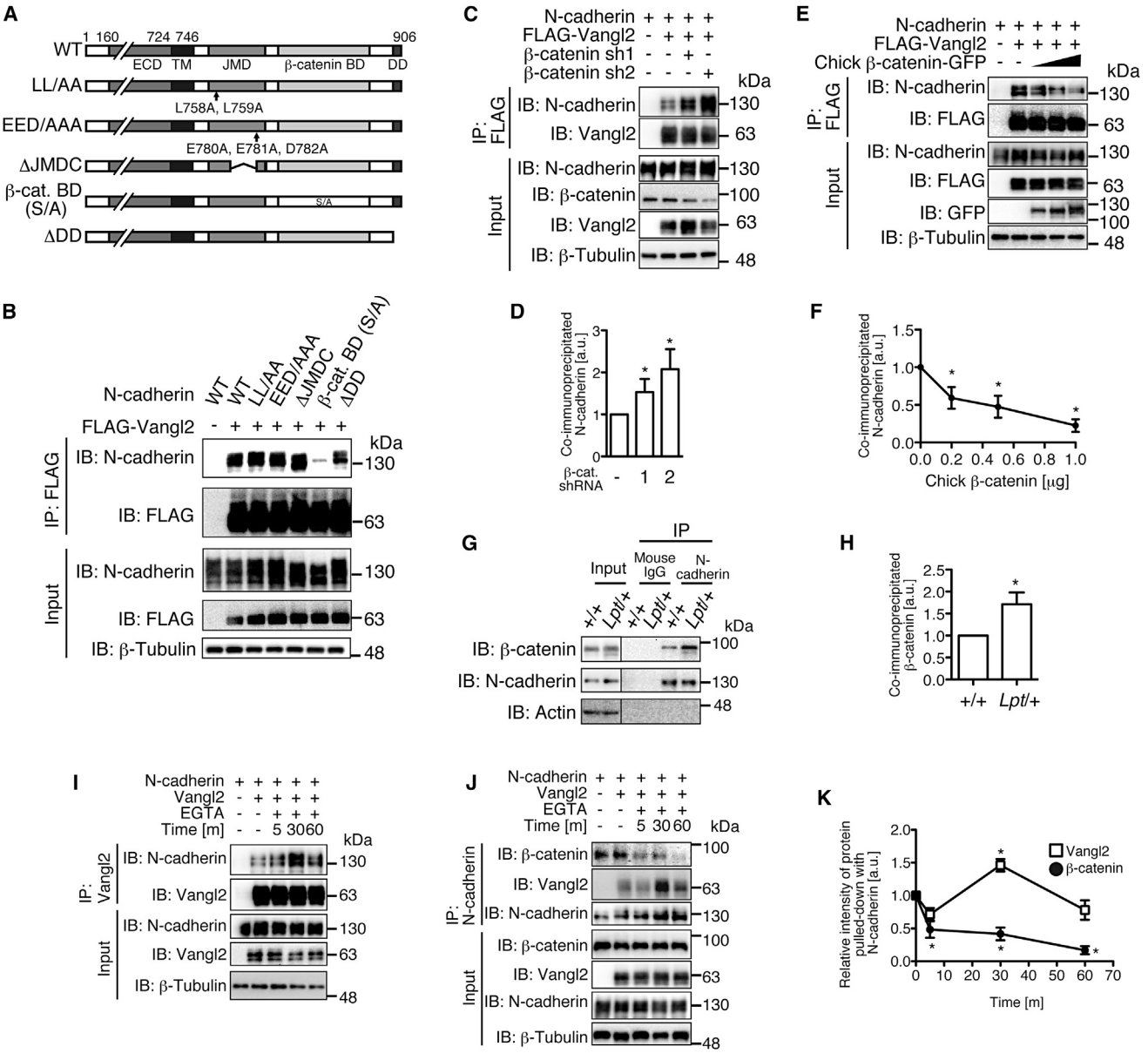

Figure 4. Interactions of Vangl2 and β-Catenin with N-Cadherin Are Mutually Exclusive

(A and B) Interaction between N-cadherin mutants and wild-type Vangl2. (A) Schematic representation of the mutant constructs. Binding was detected using WB analysis with the α-N-cadherin Abs to probe the α-FLAG IPs (B). The epitope of the α-N-cadherin Abs does not overlap with these mutated regions.

(C–F) Negative regulation of the N-cadherin-Vangl2 interaction by β-catenin. The indicated expression constructs were used to cotransfect HEK293T cells, and the immune complexes formed with FLAG-Vangl2 were subjected to WB analysis (C and E). The relative levels of IPed N-cadherin were quantified as described in the Experimental Procedures (D and F).

(G and H) Role of Vangl2 in the regulation of the N-cadherin-β-catenin interaction at the synapse. PSD fractions isolated from wild-type and *Lpt*/+ mouse brains were solubilized and IPed with the α-N-cadherin Ab. The IPs were subjected to WB analysis (G). The protein interaction was quantified as described in the Experimental Procedures (H). Note the increased level of β-catenin in the IPs from *Lpt*/+ fractions.

(I–K) EGTA dynamically changes the amounts of Vangl2 and β-catenin associated with N-cadherin. Extracts of cells treated as indicated were IPed using either α-Vangl2 (I) or α-N-cadherin (J) Abs and subjected to WB analysis. (K) Quantification of the data shown in Figure 4J. Sequential changes in the amounts of N-cadherin-bound Vangl2 (open squares) and β-catenin (filled circles) are shown in the plots. The y axis indicates the ratio of the amount of N-cadherin-bound Vangl2/β-catenin to that of the total, and the x axis indicates the time course. Note the transient increase of N-cadherin-Vangl2 interaction.

Data are presented as mean ± SD. Significant differences ($p < 0.05$) versus control groups calculated using Student's t test are marked with an asterisk.

demonstrating that the exclusive protein interaction is reflected on their functions regarding the N-cadherin transport. In this experiment, β-catenin even increased the cell-surface expression of N-cadherin, suggesting the significant basal level of N-cadherin turnover in HEK293T cells, which is sensitive to β-catenin-mediated sequestration at the cell surface. Similarly, Pk2, which perturbed the N-cadherin-Vangl2 interaction (Figure 3G), suppressed Vangl2-enhanced N-cadherin internalization (Figures 5J and 5K; Vangl2: 37.1% ± 5.5%; Vangl2 + Pk2: 79.9% ± 21.3%; Vangl2 + GFP-Pk2: 70.4% ± 11.2%), further suggesting that the physical interaction between N-cadherin and Vangl2 is essential for the Vangl2 function.

Vangl2 Regulates Cell-Surface Expression of N-Cadherin at the Synapse

To assess the significance of these results in neurons, the cell-surface expression of N-cadherin was analyzed using an N-cadherin construct with an HA tag within the ECD (Tan et al., 2010) and a GFP tag at the end of ICD (Nechiporuk et al., 2007) (HA-N-cad-GFP; Figure S5A). The cell-surface expression of this fusion protein was confirmed to be regulated similar to the wild-type N-cadherin in HEK293T cells (Figures S5B–S5D). Hippocampal neurons were cotransfected with HA-N-cad-GFP and various Vangl2 constructs and analyzed using α-HA and α-GFP Abs as described in Experimental Procedures. The cell-surface expression of N-cadherin was determined according to the ratio of fluorescence signal strengths of the α-HA and α-GFP Abs bound to each randomly selected dendritic field (>10 μm^2). The averaged ratio was significantly reduced by overexpression of wild-type Vangl2 (58.7%, 95% CI: 53.6%–64.3%; n = 20) but not by Vangl2ΔCT (103%, 95% CI: 96.2%–110%; p = 0.782; n = 20) (Figures 6A and 6B). Similarly, shRNA-mediated inhibition of Vangl2 increased the cell-surface expression of N-cadherin on the dendrites (sh1: 152%, 95% CI: 141%–164%; sh2: 135%, 95% CI: 123%–147%; n = 20 for each) (Figures 6C and 6D). When α-HA Abs were applied after permeabilization, the signal ratios were not considerably different between Vangl2-shRNA-transfected neurons and controls (Figures S5E and S5F), indicating that the α-HA Ab bound the cell-surface population of N-cadherin if applied before membrane permeabilization. Taken together, these results support the conclusion that Vangl2 at least in part regulates N-cadherin internalization at the synapse.

Because Rab5, which is associated with the N-cadherin-Vangl2 complex in HEK293T cells (Figure 5A), plays a critical role for Vangl2-enhanced internalization of N-cadherin (Figures 5F and 5G), we determined whether the association of N-cadherin with Rab5 is regulated by Vangl2 and β-catenin in the dendrites. The Vangl2- or β-catenin-shRNA-transfected neurons were immunostained with α-N-cadherin and -Rab5 Abs (Figure 6E), and their colocalization was analyzed using JACoP (Figure 6F) (Bolte and Cordelières, 2006). Pearson's coefficient, which indicates the correlation between the two immunosignals, is reduced in the Vangl2-shRNA- and conversely increased in the β-catenin-shRNA-transfected neurons (ctrl1: 0.62, 95% CI: 0.56-0.67; sh1: 0.51, 95% CI: 0.46-0.57; sh2: 0.50, 95% CI: 0.45-0.55; β-catenin-sh: 0.69, 95% CI: 0.66-0.72; n = 20 dendritic fields). These results suggest that Vangl2 and β-catenin oppositely regulate the association of N-cadherin with Rab5 and thereby determine the cell-surface expression levels of N-cadherin.

DISCUSSION

Regulation of Classic Cadherins by Vangl2

The noncanonical Wnt ligand Wnt11 regulates E-cadherin endocytosis in a Rab5c-dependent manner during zebrafish gastrulation (Ulrich et al., 2005). Further, PCP pathway-mediated cell rearrangement during epithelial tissue development in *Drosophila* requires junctional trafficking of E-cadherin (Warrington et al., 2013). In addition, zebrafish *N-cadherin* mutant exhibits abnormal tail development, which is genetically enhanced by a *Vangl2* mutation (Harrington et al., 2007). Here, we demonstrate that Vangl2 is a binding partner of N-cadherin and is involved in its internalization from the cell surface dependently on the Rab5 function. These results may explain at least one of the underlying mechanisms that link between the Wnt/PCP pathway and classic cadherin endocytosis. We further demonstrated that the N-cadherin-Vangl2 interaction is inhibited by their respective binding partners β-catenin and Pk2, suggesting that crosstalk between the cadherin-β-catenin cell adhesion system and the Strabismus/Van Gogh-Prickle PCP complex controls the transport of classic cadherins to induce precise formation and maturation of asymmetric adherens junctions such as synapse.

Vangl2 at the Synapse

Although precise control of N-cadherin trafficking at synaptic junctions plays pivotal roles in the development, functions, and plasticity of neural circuits, the regulatory mechanism remains obscure. At the postsynapse, N-cadherin is endocytosed at a high rate. However, the molecular nature of the driving force for this internalization is unknown. β-catenin inhibits this endocytosis by binding and sequestrating N-cadherin at the cell surface (Tai et al., 2007); conversely, Vangl2 is a postsynaptic factor that directly binds N-cadherin and promotes its internalization. The function of Vangl2 is competitively regulated by β-catenin; conversely, Vangl2 restricts the physical interaction between N-cadherin and β-catenin at the PSD where Vangl2 is highly concentrated. As expected, the cell-surface expression level of N-cadherin on the dendrites was affected, and the postsynaptic differentiation was impaired in neurons that expressed reduced levels of Vangl2. These results suggest that Vangl2 is one of the components that drive N-cadherin endocytosis at the postsynapses. Another postsynaptic factor known as A-kinase-anchoring protein 79/150 (AKAP 79/150), which also associates with the β-catenin binding site of N-cadherin (Gorski et al., 2005), plays a critical role in the endocytosis of AMPA receptors (Bhattacharyya et al., 2009). AKAP 79/150 might functionally interact with Vangl2 and β-catenin. In addition, Vangl2, which harbors a PDZ-binding motif, coprecipitates with PSD-95, a scaffold protein for the AMPA receptors. Further studies on the complex interactions between these molecules may reveal the mechanism of postsynaptic endocytosis, which controls synapse development and function in the CNS.

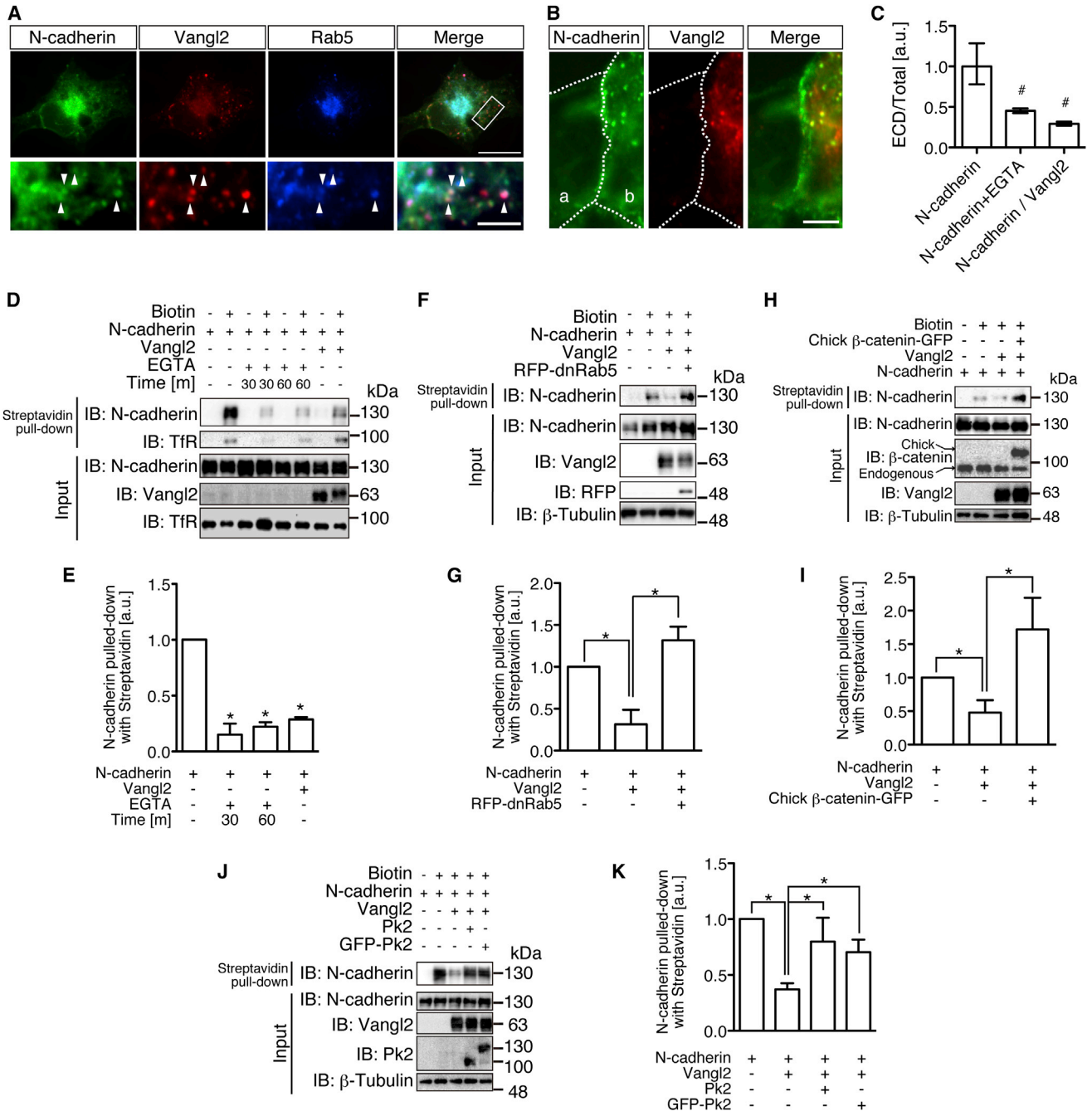

Figure 5. Vangl2 Enhances the Internalization of N-Cadherin

(A) The vesicular N-cadherin-Vangl2 complexes exhibited colocalization with Rab5 (blue) in HEK293T cells.

(B) Observation of increased N-cadherin-containing vesicles by Vangl2. MDCK cells were retransfected with Vangl2 24 hr after transfection with N-cadherin and immunostained the next day. In neighboring cells transfected with N-cadherin (a) or with both N-cadherin and Vangl2 (b), vesicular localization of N-cadherin was observed on the latter side of the border with Vangl2 colocalization. Dotted lines indicate the borders between cells.

(C) Immunofluorescence (IF) analysis of N-cadherin exposed on the cell surface. The cell-surface population was labeled with α-N-cadherin ECD Abs and the total with α-ICD Abs. The ratios of the signal intensities were indexed. Note the significant decrease of the cell-surface expression by EGTA treatment (45.3%, 95% CI: 42.5%–48.3%) or Vangl2.

(D and E) Analysis of the cell-surface expression of N-cadherin using a biotin-labeling method. Cell-surface proteins were biotinylated, bound to streptavidin beads, and quantified using WB analysis with α-N-cadherin or α-TfR Abs (D). (E) Expression level of N-cadherin on the cell surface was quantified according to the ratio of the precipitated level of N-cadherin to that of the total. Note the significant decrease of the cell-surface expression by EGTA treatment for 30 or 60 min (15.0% ± 13.9% and 22.2% ± 5.6%, respectively) or Vangl2.

(legend continued on next page)

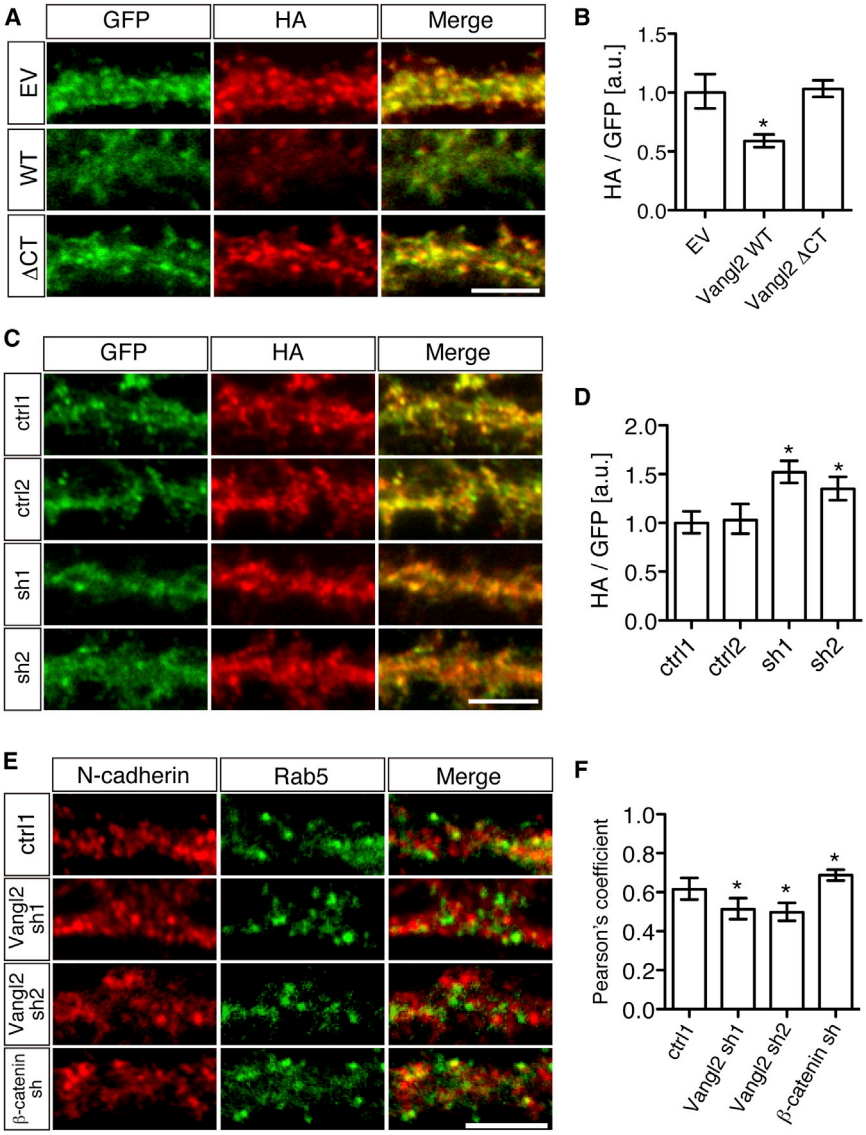

Figure 6. Abnormal Cell-Surface Expression of N-Cadherin in Neurons that Express Increased or Decreased Levels of Vangl2

(A and B) The effects of overexpression of Vangl2 or Vangl2ΔCT. The cotransfected HA-N-cad-GFP was labeled with α-HA Abs (red: middle) in the fixed neurons. After permeabilization, proteins were labeled with α-GFP Abs (green: left) (A). In this experiment, HA-N-cad-GFP did not emit significant green fluorescence without immunostaining these cultures. The cell-surface expression was quantified as described in Experimental Procedures (B). Note the reduced cell-surface expression in neurons that overexpressed wild-type Vangl2 but not Vangl2ΔCT.

(C and D) The effects of Vangl2-shRNAs on cultured neurons. Cells cotransfected with HA-N-cad-GFP were immunostained (C), and the cell-surface expression was quantified (D), as described in Figures 6A and 6B. Note the increased cell-surface expression in neurons transfected with Vangl2-shRNA.

(E and F) Association of N-cadherin with Rab5 is regulated by Vangl2 and β-catenin. Colocalization between N-cadherin and Rab5 in the dendrites of the shRNA-transfected neurons was quantified (F: y axis). Note the decreased or increased colocalization in Vangl2- or β-catenin-shRNA-transfected neurons, respectively.

Data are presented as geometric mean ± 95% CI. Significant differences ($p < 0.05$) versus control groups calculated using Mann-Whitney's U test are marked with *. a.u., arbitrary unit. Scale bars, 5 μm.

The Wnt/PCP Pathway Regulators at the Synapse

Our present results, together with those published previously (Ahmad-Annuar et al., 2006; Hida et al., 2011; Varela-Nallar et al., 2009; Yoshioka et al., 2013), lead us to hypothesize that presynaptic Fz1 and Dvl1 proteins confront postsynaptic Vangl2 and Pk2. This asymmetric pattern of protein localization across the synaptic cleft is homologous to that of Wnt/PCP-related factors at cell-cell junctions between planar polarized epithelial cells (Wallingford and Habas, 2005). In this regard, the organization of mammalian neural circuit is similar to that of the *Drosophila* wing. Fz1 and Dvl1, which function in a cell-autonomous manner as components of the canonical Wnt pathway during presynaptic differentiation (Ahmad-Annuar et al., 2006; Varela-Nallar et al., 2009), may influence signaling through the noncanonical Wnt/PCP pathway. A nonautonomous branch of the PCP pathway, which is transmitted across the cell-cell junction through direct interaction between Frizzled ectodomain ligand and Strabismus/Van Gogh transmembrane receptor, is present in *Drosophila* (Wu and Mlodzik, 2008). Future genetic studies of multiple mutant mouse strains will reveal whether postsynaptic Vangl2 and Pk2 function in

(F and G) Rab5 is required for the Vangl2-enhanced internalization of N-cadherin. The effect of dnRab5 was analyzed. WB analysis (F) and the quantification (G) are presented.

(H and I) β-catenin prevents N-cadherin internalization enhanced by Vangl2. WB analysis (H) and the quantification (I) are presented.

(J and K) Pk2 prevents N-cadherin internalization enhanced by Vangl2. Overexpression of Pk2 restored the cell-surface expression of N-cadherin. WB analysis (J) and the quantification (K) are presented.

Data are presented as mean ± SD (E, G, I, and K) or geometric mean ± 95% CI (C). Significant differences ($p < 0.05$) versus control groups calculated using Student's t test or Mann-Whitney's U test are marked with * or #, respectively. a.u., arbitrary unit. Scale bars, 20 μm (A, upper panels), 5 μm (A, lower panels), and 5 μm (B).

concert with or independently of Fz1 and Dvl1 during synapse formation.

EXPERIMENTAL PROCEDURES

Animals

Loop-tail mutants of the *LPT/Le* stock (Wilson and Center, 1977) were obtained from the Jackson Laboratory (#000220) and backcrossed to C57BL/6J mice for at least six generations. Only male mice were analyzed. The Animal Use and Care Committee of Niigata University authorized all animal experiments (permit number 111), which were performed in accordance with the National Institutes of Health *Guidelines for Care and Use of Laboratory Animals*.

Plasmids and Antibodies

The supplemental files contain detailed information on the plasmid constructs (Table S1) and Abs used in this study. The plasmid constructs were sequenced to confirm the absence of sequence errors by PCR.

Histology and Image Analysis

Immunohistochemistry, image acquisition, and quantitative analyses of signal strength were performed using the Methamorph Imaging Systems and ImageJ. Golgi staining was performed using the FD Rapid GolgiStain Kit (FD NeuroTechnologies). The cell-surface expression was quantified according to the ratio of the signal strength of the IF on the cell surface to that of the total IF. The Supplemental Information contains detailed information on the procedures of the image analysis and the Golgi staining.

Tissue Culture

HEK293T, COS7, and MDCK cells (ATCC) were maintained in standard conditions using Dulbecco's modified Eagle's medium containing GlutaMAX (Life Technologies) supplemented with 10% fetal bovine serum (BioWest) at 37°C in the presence of 5% CO_2 in a water-jacketed incubator (Napco). Rat hippocampal neurons were cultured in Neurobasal media supplemented with B27 (Brewer et al., 2008; Kaech and Banker, 2006). Transfections of the plasmid DNA were performed using Lipofectamine 2000 (Life Technologies) or Nucleofector (Lonza). The Supplemental Information contains detailed information on the procedures of culturing hippocampal neurons.

Biochemical Analysis

WB analysis and IP were conducted using standard methods. Cell fractionation of the brain homogenates was performed according to Cohen's method (Cohen et al., 1977). Protein-protein interactions determined using coIP or pull-down techniques, and the cell-surface expression of biotinylated proteins was quantified according to the ratio of the amount of precipitated protein (IP or streptavidin-pull down) to that of the total (input). The ratio of one of the control samples was set as one arbitrary unit to represent the relative amounts on the bar graphs. The Supplemental Information contains detailed information on the procedures of the biochemical analysis.

Quantification and Statistical Analysis

All counts and measurements were conducted blind. Each experiment was repeated at least twice and produced consistent results. The measured values from two independent experiments were used for each statistical analysis unless otherwise stated. The average ratio of one of the control samples (EV: empty vector, or ctrl1: control vector #1) was set as one arbitrary unit or 100% to represent the relative amounts and used as the standard for the statistical analysis.

SUPPLEMENTAL INFORMATION

Supplemental Information includes Supplemental Experimental Procedures, five figures, and one table and can be found with this article online at http://dx.doi.org/10.1016/j.celrep.2014.01.044.

AUTHOR CONTRIBUTIONS

T.N. performed all experiments. R.O. and A.I. contributed to molecular biological and histological experiments. S.S., N.F., and M.Y. bred the mice. M.I. and Y.H.H. provided support for laboratory equipment. M.K. and T.N. conceived the experiments and wrote the paper.

ACKNOWLEDGMENTS

The authors are grateful to the reviewers for their valuable comments that helped to improve the manuscript. M.K. thanks Dr. Joshua R. Sanes for his kind support during postdoctoral training, A. Watanabe, and M. Tamura for assistance, and Drs. K. Shiota, S. Nakanishi, K. Tanaka, M. Mishina, H. Okamoto, H. Nawa, R. Kageyama, K. Sakimura, R. Shigemoto, Y. Bessho, D. Watanabe, Y. Hayashi, H. Kadotani, H. Kawasaki, T. Manabe, K. Tabuchi, N. Takei, and the members of the tenure-track committee of the Niigata University for encouragement.

Received: May 21, 2013
Revised: January 17, 2014
Accepted: January 31, 2014
Published: February 27, 2014

REFERENCES

Ahmad-Annuar, A., Ciani, L., Simeonidis, I., Herreros, J., Fredj, N.B., Rosso, S.B., Hall, A., Brickley, S., and Salinas, P.C. (2006). Signaling across the synapse: a role for Wnt and Dishevelled in presynaptic assembly and neurotransmitter release. J. Cell Biol. *174*, 127–139.

Arikkath, J., and Reichardt, L.F. (2008). Cadherins and catenins at synapses: roles in synaptogenesis and synaptic plasticity. Trends Neurosci. *31*, 487–494.

Bhattacharyya, S., Biou, V., Xu, W., Schlüter, O., and Malenka, R.C. (2009). A critical role for PSD-95/AKAP interactions in endocytosis of synaptic AMPA receptors. Nat. Neurosci. *12*, 172–181.

Biederer, T., Sara, Y., Mozhayeva, M., Atasoy, D., Liu, X., Kavalali, E.T., and Südhof, T.C. (2002). SynCAM, a synaptic adhesion molecule that drives synapse assembly. Science *297*, 1525–1531.

Bohdanowicz, M., Balkin, D.M., De Camilli, P., and Grinstein, S. (2012). Recruitment of OCRL and Inpp5B to phagosomes by Rab5 and APPL1 depletes phosphoinositides and attenuates Akt signaling. Mol. Biol. Cell *23*, 176–187.

Bolte, S., and Cordelières, F.P. (2006). A guided tour into subcellular colocalization analysis in light microscopy. J. Microsc. *224*, 213–232.

Brewer, G.J., Boehler, M.D., Jones, T.T., and Wheeler, B.C. (2008). NbActiv4 medium improvement to Neurobasal/B27 increases neuron synapse densities and network spike rates on multielectrode arrays. J. Neurosci. Methods *170*, 181–187.

Bucci, C., Parton, R.G., Mather, I.H., Stunnenberg, H., Simons, K., Hoflack, B., and Zerial, M. (1992). The small GTPase rab5 functions as a regulatory factor in the early endocytic pathway. Cell *70*, 715–728.

Cohen, R.S., Blomberg, F., Berzins, K., and Siekevitz, P. (1977). The structure of postsynaptic densities isolated from dog cerebral cortex. I. Overall morphology and protein composition. J. Cell Biol. *74*, 181–203.

Devenport, D., Oristian, D., Heller, E., and Fuchs, E. (2011). Mitotic internalization of planar cell polarity proteins preserves tissue polarity. Nat. Cell Biol. *13*, 893–902.

Elia, L.P., Yamamoto, M., Zang, K., and Reichardt, L.F. (2006). p120 catenin regulates dendritic spine and synapse development through Rho-family GTPases and cadherins. Neuron *51*, 43–56.

Ferrer, I., and Gullotta, F. (1990). Down's syndrome and Alzheimer's disease: dendritic spine counts in the hippocampus. Acta Neuropathol. *79*, 680–685.

Firestein, R., Bass, A.J., Kim, S.Y., Dunn, I.F., Silver, S.J., Guney, I., Freed, E., Ligon, A.H., Vena, N., Ogino, S., et al. (2008). CDK8 is a colorectal cancer oncogene that regulates beta-catenin activity. Nature *455*, 547–551.

Gorski, J.A., Gomez, L.L., Scott, J.D., and Dell'Acqua, M.L. (2005). Association of an A-kinase-anchoring protein signaling scaffold with cadherin adhesion molecules in neurons and epithelial cells. Mol. Biol. Cell *16*, 3574–3590.

Graf, E.R., Zhang, X., Jin, S.X., Linhoff, M.W., and Craig, A.M. (2004). Neurexins induce differentiation of GABA and glutamate postsynaptic specializations via neuroligins. Cell *119*, 1013–1026.

Gravel, M., Iliescu, A., Horth, C., Apuzzo, S., and Gros, P. (2010). Molecular and cellular mechanisms underlying neural tube defects in the loop-tail mutant mouse. Biochemistry *49*, 3445–3455.

Guyot, M.C., Bosoi, C.M., Kharfallah, F., Reynolds, A., Drapeau, P., Justice, M., Gros, P., and Kibar, Z. (2011). A novel hypomorphic Looptail allele at the planar cell polarity Vangl2 gene. Developmental dynamics: an official publication of the American Association of Anatomists *240*, 839–849.

Harrington, M.J., Hong, E., Fasanmi, O., and Brewster, R. (2007). Cadherin-mediated adhesion regulates posterior body formation. BMC Dev. Biol. *7*, 130.

Hida, Y., Fukaya, M., Hagiwara, A., Deguchi-Tawarada, M., Yoshioka, T., Kitajima, I., Inoue, E., Watanabe, M., and Ohtsuka, T. (2011). Prickle2 is localized in the postsynaptic density and interacts with PSD-95 and NMDA receptors in the brain. J. Biochem. *149*, 693–700.

Jenny, A., Darken, R.S., Wilson, P.A., and Mlodzik, M. (2003). Prickle and Strabismus form a functional complex to generate a correct axis during planar cell polarity signaling. EMBO J. *22*, 4409–4420.

Kaech, S., and Banker, G. (2006). Culturing hippocampal neurons. Nat. Protoc. *1*, 2406–2415.

Kibar, Z., Underhill, D.A., Canonne-Hergaux, F., Gauthier, S., Justice, M.J., and Gros, P. (2001a). Identification of a new chemically induced allele (*Lp*(*m1Jus*)) at the *loop-tail* locus: morphology, histology, and genetic mapping. Genomics *72*, 331–337.

Kibar, Z., Vogan, K.J., Groulx, N., Justice, M.J., Underhill, D.A., and Gros, P. (2001b). *Ltap*, a mammalian homolog of Drosophila Strabismus/Van Gogh, is altered in the mouse neural tube mutant *Loop-tail*. Nat. Genet. *28*, 251–255.

Le, T.L., Yap, A.S., and Stow, J.L. (1999). Recycling of E-cadherin: a potential mechanism for regulating cadherin dynamics. J. Cell Biol. *146*, 219–232.

Miyashita, Y., and Ozawa, M. (2007). A dileucine motif in its cytoplasmic domain directs beta-catenin-uncoupled E-cadherin to the lysosome. J. Cell Sci. *120*, 4395–4406.

Murase, S., Mosser, E., and Schuman, E.M. (2002). Depolarization drives beta-Catenin into neuronal spines promoting changes in synaptic structure and function. Neuron *35*, 91–105.

Nechiporuk, T., Fernandez, T.E., and Vasioukhin, V. (2007). Failure of epithelial tube maintenance causes hydrocephalus and renal cysts in Dlg5-/- mice. Dev. Cell *13*, 338–350.

Okabe, S. (2012). Molecular dynamics of the excitatory synapse. Adv. Exp. Med. Biol. *970*, 131–152.

Perez-Cruz, C., Nolte, M.W., van Gaalen, M.M., Rustay, N.R., Termont, A., Tanghe, A., Kirchhoff, F., and Ebert, U. (2011). Reduced spine density in specific regions of CA1 pyramidal neurons in two transgenic mouse models of Alzheimer's disease. J. Neurosci. *31*, 3926–3934.

Scheiffele, P., Fan, J., Choih, J., Fetter, R., and Serafini, T. (2000). Neuroligin expressed in nonneuronal cells triggers presynaptic development in contacting axons. Cell *101*, 657–669.

Segal, M. (2005). Dendritic spines and long-term plasticity. Nat. Rev. Neurosci. *6*, 277–284.

Shafer, B., Onishi, K., Lo, C., Colakoglu, G., and Zou, Y. (2011). Vangl2 promotes Wnt/planar cell polarity-like signaling by antagonizing Dvl1-mediated feedback inhibition in growth cone guidance. Dev. Cell *20*, 177–191.

Stappert, J., and Kemler, R. (1994). A short core region of E-cadherin is essential for catenin binding and is highly phosphorylated. Cell Adhes. Commun. *2*, 319–327.

Strutt, D., and Strutt, H. (2007). Differential activities of the core planar polarity proteins during Drosophila wing patterning. Dev. Biol. *302*, 181–194.

Suzuki, M., Van Paesschen, W., Stalmans, I., Horita, S., Yamada, H., Bergmans, B.A., Legius, E., Riant, F., De Jonghe, P., Li, Y., et al. (2010). Defective membrane expression of the Na(+)-HCO(3)(-) cotransporter NBCe1 is associated with familial migraine. Proc. Natl. Acad. Sci. USA *107*, 15963–15968.

Tai, C.Y., Mysore, S.P., Chiu, C., and Schuman, E.M. (2007). Activity-regulated N-cadherin endocytosis. Neuron *54*, 771–785.

Takahashi, H., Arstikaitis, P., Prasad, T., Bartlett, T.E., Wang, Y.T., Murphy, T.H., and Craig, A.M. (2011). Postsynaptic TrkC and presynaptic PTPσ function as a bidirectional excitatory synaptic organizing complex. Neuron *69*, 287–303.

Takeichi, M., and Abe, K. (2005). Synaptic contact dynamics controlled by cadherin and catenins. Trends Cell Biol. *15*, 216–221.

Tan, Z.J., Peng, Y., Song, H.L., Zheng, J.J., and Yu, X. (2010). N-cadherin-dependent neuron-neuron interaction is required for the maintenance of activity-induced dendrite growth. Proc. Natl. Acad. Sci. USA *107*, 9873–9878.

Tissir, F., and Goffinet, A.M. (2006). Expression of planar cell polarity genes during development of the mouse CNS. Eur. J. Neurosci. *23*, 597–607.

Togashi, H., Abe, K., Mizoguchi, A., Takaoka, K., Chisaka, O., and Takeichi, M. (2002). Cadherin regulates dendritic spine morphogenesis. Neuron *35*, 77–89.

Ulrich, F., Krieg, M., Schötz, E.M., Link, V., Castanon, I., Schnabel, V., Taubenberger, A., Mueller, D., Puech, P.H., and Heisenberg, C.P. (2005). Wnt11 functions in gastrulation by controlling cell cohesion through Rab5c and E-cadherin. Dev. Cell *9*, 555–564.

Varela-Nallar, L., Grabowski, C.P., Alfaro, I.E., Alvarez, A.R., and Inestrosa, N.C. (2009). Role of the Wnt receptor Frizzled-1 in presynaptic differentiation and function. Neural Dev. *4*, 41.

Wallingford, J.B., and Habas, R. (2005). The developmental biology of Dishevelled: an enigmatic protein governing cell fate and cell polarity. Development *132*, 4421–4436.

Warrington, S.J., Strutt, H., and Strutt, D. (2013). The Frizzled-dependent planar polarity pathway locally promotes E-cadherin turnover via recruitment of RhoGEF2. Development *140*, 1045–1054.

Willingham, M.C. (2010). Fluorescence labeling of surface antigens of attached or suspended tissue-culture cells. Methods Mol. Biol. *588*, 143–151.

Wilson, D.B., and Center, E.M. (1977). Differences in cerebral morphology in 2 stocks of mutant mice heterozygous for the loop-tail (*Lp*)-gene. Experientia *33*, 1502–1503.

Wu, J., and Mlodzik, M. (2008). The frizzled extracellular domain is a ligand for Van Gogh/Stbm during nonautonomous planar cell polarity signaling. Dev. Cell *15*, 462–469.

Yin, H., Copley, C.O., Goodrich, L.V., and Deans, M.R. (2012). Comparison of phenotypes between different *vangl2* mutants demonstrates dominant effects of the *Looptail* mutation during hair cell development. PLoS ONE *7*, e31988.

Yoshihara, Y., De Roo, M., and Muller, D. (2009). Dendritic spine formation and stabilization. Curr. Opin. Neurobiol. *19*, 146–153.

Yoshioka, T., Hagiwara, A., Hida, Y., and Ohtsuka, T. (2013). Vangl2, the planner cell polarity protein, is complexed with postsynaptic density protein PSD-95. FEBS Lett. *587*, 1453–1459.

Zhou, L., Bar, I., Achouri, Y., Campbell, K., De Backer, O., Hebert, J.M., Jones, K., Kessaris, N., de Rouvroit, C.L., O'Leary, D., et al. (2008). Early forebrain wiring: genetic dissection using conditional *Celsr3* mutant mice. Science *320*, 946–949.